

Stability of HSQ nanolines defined by e-beam lithography for Si nanowire field effect transistors

Suresh Regonda, Mukti Aryal, and Wenchuang (Walter) Hu^{a)}

Department of Electrical Engineering, University of Texas at Dallas, Richardson, Texas 75080

(Received 17 June 2008; accepted 22 September 2008; published 1 December 2008)

Multiple instability states, e.g., grouped collapse, single collapse, wavy, and grouped wavy states, have been observed in hydrogen silses quioxane (HSQ) nanolines defined by electron beam lithography (EBL). Experimental data show that the critical aspect ratio of the HSQ lines dramatically increase when the line pitch reduced to sub-100-nm, which is opposite to theoretical models for capillary forces and swelling strain. Such contradiction can be well explained only if Young's modulus is considered as a significantly varying factor. Further, experimental data show a dramatic decrease in swelling strain and increase in oxygen contents in HSQ with increasing EBL dose, indicating that it is the change in Young's modulus rather than the capillary force or swelling strain that dominates the instability behaviors at the nanoscale. Stable high aspect ratio HSQ nanolines over metal pads were used to make working Si nanowire transistors on Si on insulator substrates. 12–14 nm HSQ lines with aspect ratios of 11–14 have been obtained. Fabricated field effect transistors using back-gate configuration has shown expected performance towards biosensing applications. © 2008 American Vacuum Society. [DOI: 10.1116/1.3002561]

I. INTRODUCTION

The stability of nanoscale resist patterns defined by lithography is an important issue for the fabrication of nanodevices and systems.^{1–3} High aspect ratio resist patterns are favorable for etching, lift-off, and across step heights. In many cases, it is actually not the lithography process but the instability issues of photoresist that limit the optimal aspect ratio. Several studies have been reported on the resist mechanical properties and its instability behaviors.^{4–8} However, comprehensive understanding of complex instability behavior is still quite limited, particularly at the nanoscale. In addition, most of the studies are focused on positive resists such as polymethyl methacrylate where Young's modulus is relatively constant. For most negative resists such as hydrogen silses quioxane (HSQ), mechanical properties can significantly differ for varying cross-linking degrees. HSQ has become a popular negative inorganic resist for e-beam lithography (EBL) due to its capability for sub-10-nm resolution, small line edge roughness, high etch resistance, and good mechanical strength.^{9,10} HSQ has been used widely to fabricate nanowire devices for logic computing and biochemical sensing.^{11–14} In-depth understanding of resist stability is important to optimize nanofabrication processes.

Here, we present a study of correlations among the instability behaviors of HSQ lines, exposure dose, cross-linking degree, geometry, capillary force, and swelling strain from the development and rinse processes.

II. EXPERIMENTS

A. Sample preparation

HSQ (Fox-12, Dow Corning Co.) with thicknesses of 60, 130, and 180 nm was spin coated on Si and Si on insulator

(SOI) substrates, followed by soft bake at 140 °C on a hot plate for 180 s. EBL was then performed on a Zeiss Supra 40 scanning electron microscopy (SEM) with a Naby pattern generator. 30 kV accelerating voltage and 20–250 pA beam current were used to expose a matrix of gratings of various pitches and doses. After EBL, HSQ was developed in 25 wt % tetramethyl-ammonium-hydroxide for 60 s at a temperature of 50 °C.

B. Observation of HSQ instability behaviors

Figure 1 shows 45° tilted SEM views of four typical instability states of HSQ nanolines: stable, single and grouped collapse, and wavy nanolines, respectively. For all different grating pitches, it was observed universally that the instability states always transit from poorly resolved lines, to wavy, then to collapsed, and finally reaching stable lines with increasing doses. For each HSQ thickness (H) of 60, 130, and 180 nm, linewidths (W) were measured and aspect ratios of the lines were calculated by $AR=H/W$. The critical aspect ratio {CAR} is defined as the maximum achievable aspect ratio of stable lines for a given pitch and dose. Figure 2(a) plots the CAR as a function of line pitch for the three HSQ thicknesses. The doses for each data point describe the boundary conditions that differentiate stable and unstable lines, which are different for different pitches. For both 130 and 180 nm thick HSQ lines, CAR increases dramatically when decreasing pitch within the sub-100-nm region. As will be discussed later, this is opposite to the previous observation and models.^{6–8} The CAR for 60 nm thick lines is almost constant for varying pitches. This is because the thin HSQ thickness limits the maximum aspect ratio that can be obtained under current EBL system constrains of resolution. Figure 1(e) shows 12 nm wide lines of 11 aspect ratio and 50 nm pitch. Figure 2(b) shows the CAR versus dose for

^{a)}Electronic mail: walter.hu@utdallas.edu

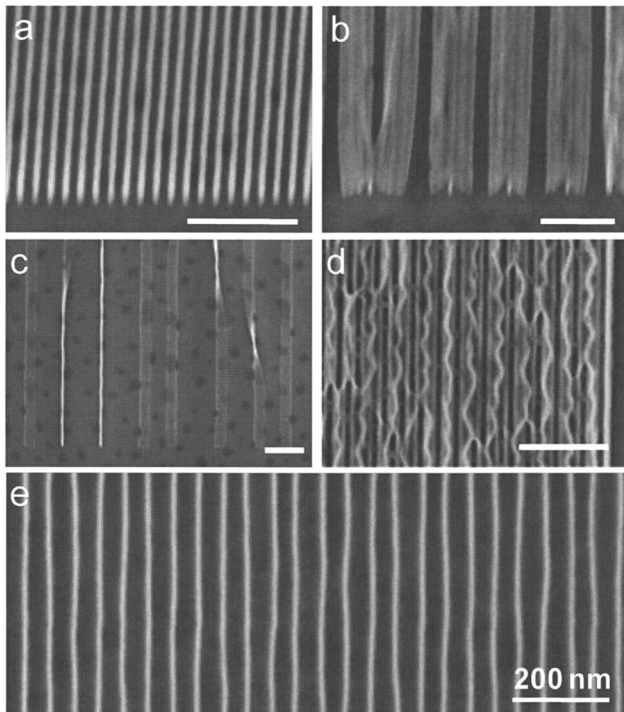


FIG. 1. SEM 45° tilted view of HSQ lines in four stability states: (a) stable, (b) clustering or grouped collapsed lines, (c) completely collapsed lines forming free ribbons on the surface, (d) wavy lines with a spatial wavelength of 150–200 nm; and (e) 12 nm wide lines of 50 nm pitch and aspect ratio of 11. Scale bar in images (a)–(d) is 500 nm.

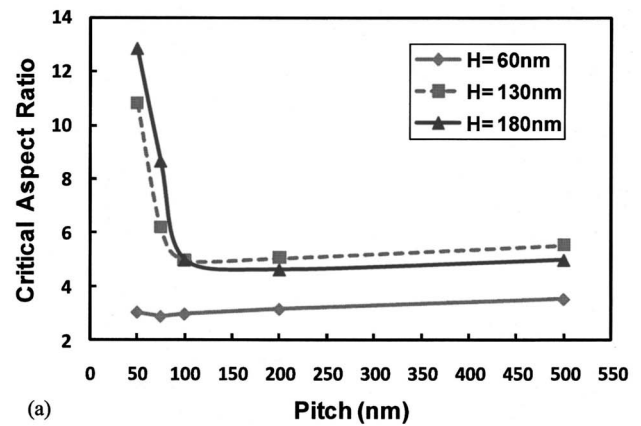
three different pitches. It indicates that a larger dose allows a higher aspect ratio, which will be discussed further in Sec. III.

C. Analysis of HSQ cross-linking

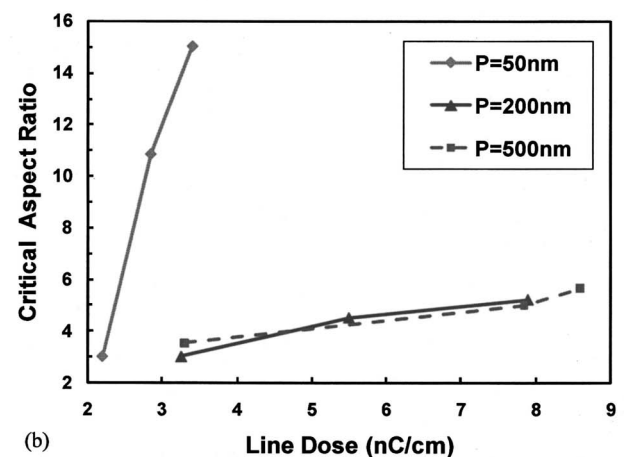
A HSQ square array of $2 \times 2 \mu\text{m}^2$ in size, 180 nm in height, and $20 \mu\text{m}$ in spacing, with gradually increasing dose from 300 to $1020 \mu\text{C}/\text{cm}^2$, were defined by EBL on a Si substrate. After development, the square array was analyzed using energy dispersive analysis of x rays (EDAX) in a SEM to quantify the relative amounts of oxygen and Si in the HSQ for varying doses. The oxygen percentage relative to Si measured by EDAX indicates the Si–O bonds in the HSQ, which represents its cross-linking degree due to e-beam exposure. Figure 3 shows the amount of oxygen as a function of exposure dose. It is clearly observed that increasing dose results in a significant increase in cross-linking at 300–600 $\mu\text{C}/\text{cm}^2$ and saturates after 600 $\mu\text{C}/\text{cm}^2$. Please note that the oxygen percentage in Fig. 3 is lower than the true Si–O bonds in HSQ because EDAX was performed at 5 kV which picks up a larger amount of Si from the substrate in addition to HSQ.

III. MODELING AND DISCUSSIONS

It is believed that the deformation of resist lines is due to liquid induced capillary forces, swelling strain, dewetting, and pattern geometry constrains during the development, rinse, and drying processes. Previously, several models and



(a)



(b)

FIG. 2. Critical aspect ratio as a function of (a) grating pitch and (b) e-beam exposure dose for HSQ lines of three thicknesses: 60, 130, and 180 nm.

techniques were developed to study the mechanical properties of resist patterns, such as beam bending model^{7,8} and linear plate deformation model.¹⁵ Critical aspect ratio as a function of line geometry (pitch, width, spacing, etc.) has been studied.^{5,6} Since positive resists were used in these studies, Young's modulus E was treated as a relatively constant factor. In this study, we found that the combination of

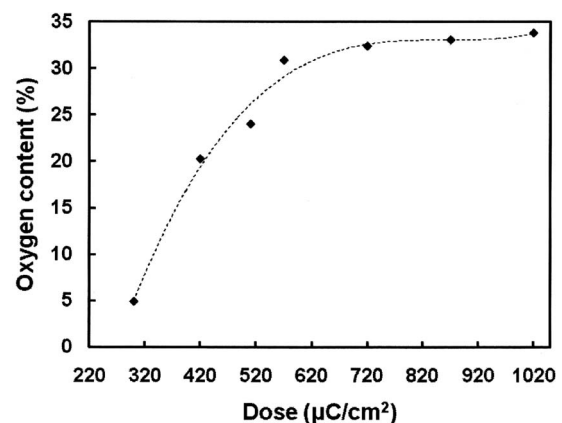


FIG. 3. Oxygen content in 180 nm thick HSQ squares on Si as a function of area dose.

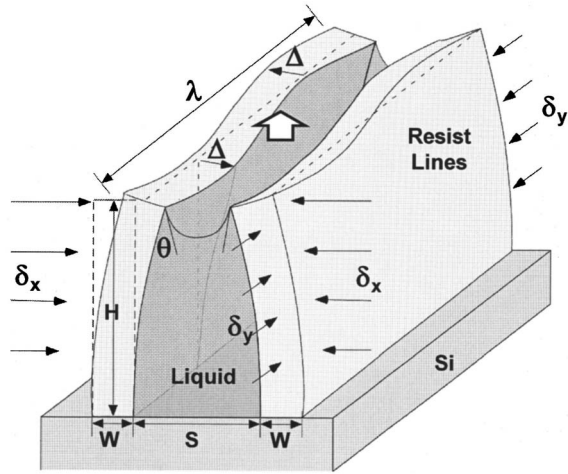


FIG. 4. Schematic of line instability model combining the effect of capillary forces and swelling strain.

linear plate model and beam bending model is necessary to explain the complex instability behaviors of HSQ lines. Young's modulus of the HSQ lines is treated as a function of given doses and geometry. Figure 4 shows the schematic of the resist models, which contain two resist lines separated by a space S or $pitch = W + S$. Capillary force from liquid induces bending deformation (δ_x) perpendicular to the line walls. On the other hand, resist swelling of liquid causes strains in both the x and y directions, resulting in wavy deformation with amplitude (Δ) in the x direction, a spatial wavelength of λ , and lateral displacement deformation (δ_y), respectively. Swelling strain can be estimated as¹⁵

$$\varepsilon_{sw} = \left(\frac{\pi\Delta}{\lambda}\right)^2 \left[1 - \frac{3}{2}\left(\frac{\pi\Delta}{\lambda}\right)^2\right]. \quad (1)$$

Both Δ and λ were measured on the wavy lines and swelling strain was calculated as a function of dose, as shown in Fig. 5. The swelling strain rapidly decreases when the exposure dose increases above 1.7 nC/cm. Lines of dose higher than 1.8 nC/cm do not appear to have wavy instability behavior. It is known that HSQ undergoes cage network structural transformation during e-beam exposure or thermal curing due to the conversion of Si-H bonds to Si-O bonds.^{16,17}

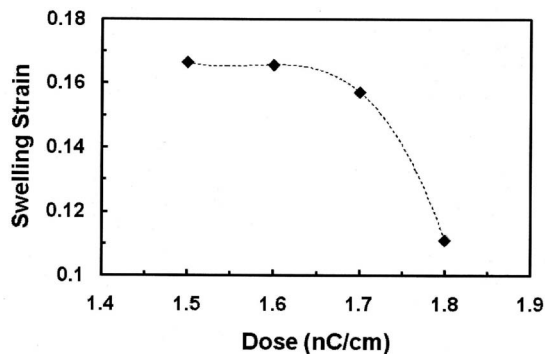


FIG. 5. Swelling strain of wavy HSQ lines of 180 nm thickness as a function of line dose.

Lightly exposed HSQ will have more Si-H bonds than highly exposed HSQ. Since the developer reacts with Si-H bonds and not Si-O bonds, it will have the tendency to penetrate into lightly exposed patterns, causing the swelling of HSQ resists. So, the swelling behavior can be more prominent in less exposed patterns than highly exposed ones.

The maximum line-wall bending due to capillary forces can be estimated as⁸

$$\delta_{x\text{-max}} = \frac{3H(AR)^3\gamma\cos\theta}{SE}, \quad (2)$$

where γ , θ , and E are the surface tension of liquid, contact angle of liquid on resist line walls, and Young's modulus of resist. Such deformation above a threshold value will cause lines to collapse together or individually as shown in Figs. 1(b) and 1(c). The critical aspect ratio can be derived from Eq. (2) as

$$CAR = \left(\frac{SE\alpha}{3\gamma\cos\theta}\right)^{1/3}, \quad (3)$$

where $\alpha = \tan^{-1}(\delta_{x\text{-max}}/H) \approx \delta_{x\text{-max}}/H$ is the bending angle of resist lines. For stable lines, line bending angle α is very small. Based on Eq. (3), CAR should decrease with decreasing line spacing S or line pitch, as observed previously where E is assumed as relatively constant.^{5,6,8} Our measurement data in Fig. 2(a) also show this trend when the pitch is larger than 100 nm. However, the trend becomes strongly opposite when pitch decreases to sub-100-nm, indicating a much faster increase in E than a decrease in S . EBL simulation using two Gaussian models (results not shown) has shown that the effective dose for gratings significantly increases when pitch is smaller than 100 nm at 30 kV due to proximity effect. Therefore, one explanation of Fig. 2(a) is that the decrease in pitch increases the effective dose, resulting in a dramatic increase in E . In Fig. 2(b), for the same pitch, increasing dose results in a higher CAR. Please note that for larger pitches, the CAR is not as high as smaller pitches because significantly higher doses are needed to achieve line stability, which results in wider lines for limited thin HSO resist. The results indicate that it is Young's modulus that dominates the effects on CAR and line stability and not the capillary forces from solution at this length scale.

To further quantify the effects of exposure dose on HSQ cross-linking and Young's modulus, we performed the EDAX experiment as shown in Fig. 3. Oxygen content does increase rapidly around a threshold dose of $\sim 300 \mu\text{C}/\text{cm}^2$ and then saturated at a dose $\sim 600 \mu\text{C}/\text{cm}^2$. Previous experimental studies show that Young's modulus of resist increases exponentially when the Si-O/Si-H ratio increases.^{17,18} These experiments prove that cross-linking of HSQ can significantly affect its Young's modulus and therefore instability behaviors particularly at the sub-100-nm region. This may be true for other negative resists as well.

What we can learn from this is that to achieve optimum aspect ratio patterns in negative resists at the nanoscale, the geometry design may not be important to offset capillary effects but the control of exposure dose and resist curing. For

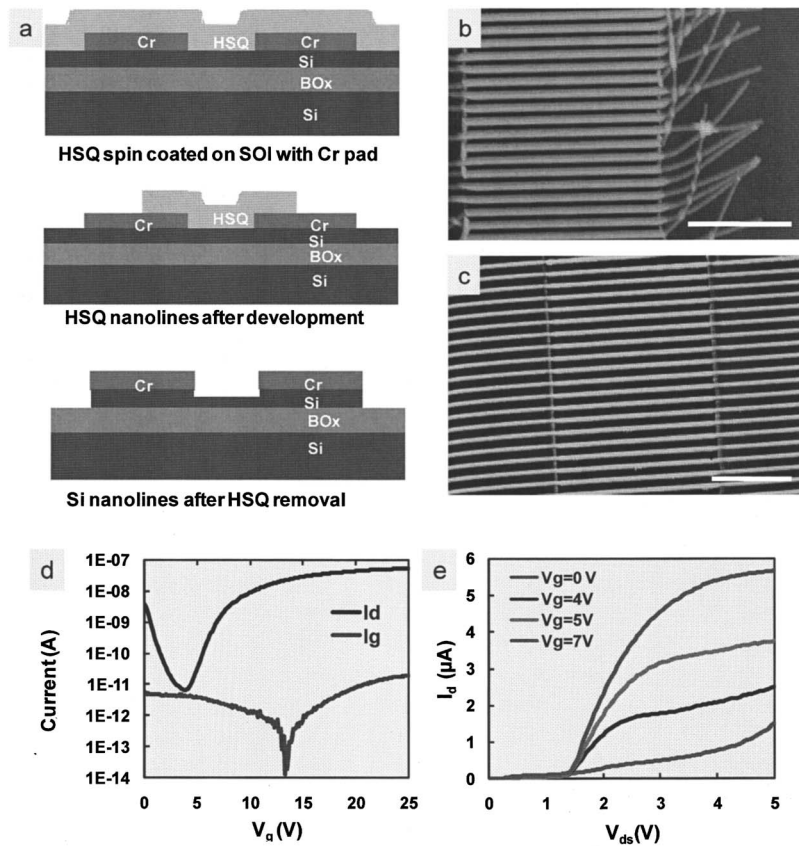


FIG. 6. (a) Schematic of the fabrication process of Si nanowire FETs. (b) atomic force microscopy image of 100 nm HSQ lines crossing the gap between two Cr pads, showing the line peeling-off problem; scale bar is 2 μm . (c) 180 nm HSQ lines across the step of Cr pads without instability issues; scale bar is 2 μm . (d) I_d - V_g curve of SiNW FETs with 50 nm wide, 4 μm long Si channels. The device contains 12 lines crossing the gap and source-drain bias is 0.25 V. (e) I_d - V_{ds} curve of the same device with several different V_g .

ultrasmall and stable patterns, a good strategy may be to choose a high dose for good stability and optimize development to obtain narrow dimensions.^{19–22} For high density patterns, we have observed nonuniform instability behaviors due to varying effective exposure doses. Correction of proximity effect can be used to alleviate these issues not only for uniform dimensions but also for uniform pattern stability.

IV. APPLICATION IN SI NANOWIRE TRANSISTORS

We intend to transfer stable HSQ nanolines to SOI substrates to make Si nanowire (SiNW) field effect transistors (FETs) for electronic sensing of biomolecules, as shown in Fig. 6(a). For biosensing applications, back Si substrate was used as gate and buried oxide (BOx) as gate dielectric layer, leaving the Si nanowires channel open to analyte solution. SOI wafer has a 70 nm thick Si layer on a 145 nm BOx. Si was doped with boron at a level of 10^{15} cm^{-3} . No source/drain doping is used and the FETs function in ambipolar accumulation modes. 100 nm thick Cr contacts were first patterned on SOI separated with 2–10 μm gaps. HSQ was spin coated onto the wafer and EBL was used to define nanolines across the Cr pads. After HSQ lines were developed, they were used as a mask for plasma etching of Si using Cl_2 chemistry (Inductively Coupled Plasma power of 150 W, rf power of 50 W, 5 mTorr). HSQ was removed with 20:1 buffered oxide etch solution and then devices were characterized on a probe station.

For the device fabrication, we first used thin HSQ (60–130 nm in thickness) on Cr so as to achieve the narrowest possible lines. It was found that HSQ nanolines show poor stability across the Cr pads. As shown in Fig. 6(b), the poor step coverage results in HSQ peeling-off from the Cr pads. Based on the studies of stability, we figured out that the use of a high dose and thick HSQ (180 nm) can achieve high aspect ratio lines. The experimental result in Fig. 6(c) demonstrates that high aspect ratio lines were able to form excellent step coverage and maintain their stability on Cr pads. HSQ lines as small as 17 nm wide and 180 nm tall have been demonstrated on Cr pads.

Figures 6(d) and 6(e) show expected electronic characterization curves of SiNW FETs. The on/off ratio of the FET is $\sim 10\,000$, gate leakage current is less than 0.1 pA, and threshold voltage is ~ 7.6 V. Drain current as a function of source-drain bias shows clear linear and saturation regions. Please note that the I_g in Fig. 6(d) was 1–10 pA mostly. This is not gate leakage but displacement current during biasing the huge Si back gate. With the use of stable high aspect ratio HSQ lines, this desired device process is successful.

V. CONCLUSIONS

Multiple instability states (wavy, collapse, or their combination) of EBL defined HSQ nanolines have been observed experimentally as functions of line pitch, dose, and height. The critical aspect ratios of HSQ lines dramatically increase when the line pitch reduced to sub-100-nm. A model com-

binning beam bending and linear plate was used to analyze the correlations among instability behaviors, capillary forces, swelling strain, line geometry, and Young's modulus. The model explains well the observed instability behaviors only if Young's modulus is considered as a significantly varying factor. Experimental data show a dramatic decrease in swelling strain and increase in oxygen contents in HSQ with increasing EBL dose. These new observations indicate that it is the change in Young's modulus rather than the capillary force or swelling strain that dominates the instability behaviors at the nanoscale for negative resist patterns.

Stable high aspect ratio HSQ nanolines enable excellent step coverage over metal pads to make Si nanowire transistors. 12–17 nm HSQ lines with aspect ratio of 12–14 have been obtained. Fabricated Si nanowire FETs using back-gate configuration has shown expected performance towards biosensing applications.

ACKNOWLEDGMENTS

The authors would like to thank Eric M. Vogel, Nikki Fernandes, Ram Pratiwadi, and Kurtis Cantley at The University of Texas at Dallas for discussion on device fabrication and help on device characterization. This work is partially supported by a subcontract from Lynntech, Texas and funding from Texas Instruments Inc., Richardson, Texas.

¹K. Deguchi, K. Miyoshi, T. Ishii, and T. Matsuda, *Jpn. J. Appl. Phys.*, Part 1 **31**, 2954 (1992).

²H. Namatsu, M. Nagase, K. Kurihara, K. Iwadate, T. Furuta, and K. Murase, *Microelectron. Eng.* **27**, 71 (1995).

³H. Namatsu, Y. Yamazaki, T. Yamaguchi, M. Nagase, and K. Kurihara, *J. Vac. Sci. Technol. B* **16**, 69 (1998).

⁴M. Kotera and N. Ochiai, *Microelectron. Eng.* **78–79**, 515 (2005).

⁵M. P. Stoykovich, H. B. Cao, K. Yoshimoto, L. E. Ocola, and P. F. Nealey, *Adv. Mater. (Weinheim, Ger.)* **15**, 1180 (2003).

⁶M. P. Stoykovich, K. Yoshimoto, and P. F. Nealey, *Appl. Phys. A: Mater. Sci. Process.* **90**, 277 (2008).

⁷T. Tanaka, M. Morigami, and N. Atoda, *Jpn. J. Appl. Phys.*, Part 1 **32**, 6059 (1993).

⁸K. Yoshimoto, M. P. Stoykovich, H. B. Cao, J. J. de Pablo, and P. F. Nealey, *J. Appl. Phys.* **96**, 1857 (2004).

⁹K. A. Lister, B. G. Casey, P. S. Dobson, S. Thoms, D. S. Macintyre, C. D. W. Wilkinson, and J. M. R. Weaver, *Microelectron. Eng.* **73–74**, 319 (2004).

¹⁰H. Namatsu, T. Yamaguchi, M. Nagase, Y. Yamazaki, and K. Kurihara, *Microelectron. Eng.* **42**, 331 (1998).

¹¹O. H. Elibol, D. Morissette, D. Akin, J. P. Denton, and R. Bashir, *Appl. Phys. Lett.* **83**, 4613 (2003).

¹²Z. Li, Y. Chen, X. Li, T. I. Kamins, K. Nauka, and R. S. Williams, *Nano Lett.* **4**, 245 (2004).

¹³Z. Li, B. Rajendran, T. I. Kamins, X. Li, Y. Chen, and R. S. Williams, *Appl. Phys. A: Mater. Sci. Process.* **80**, 1257 (2005).

¹⁴K. Sang-Mo, M. D. Edelstein, Q. Li, C. A. Richter, and E. M. Vogel, *Nanotechnology* **16**, 1482 (2005).

¹⁵X. Huang, G. Bazan, D. A. Hill, and G. H. Bernstein, *J. Electrochem. Soc.* **139**, 5 (1992).

¹⁶C. C. Yang and W. C. Chen, *J. Mater. Chem.* **12**, 1138 (2002).

¹⁷J. K. W. Yang, V. Anant, and K. K. Berggren, *J. Vac. Sci. Technol. B* **24**, 5 (2006).

¹⁸H. C. Liou and J. Pretzer, *Thin Solid Films* **335**, 186 (1998).

¹⁹Y. F. Chen, H. F. Yang, and Z. Cui, *Microelectron. Eng.* **83**, 1119 (2006).

²⁰W. C. Hu, K. Sarveswaran, M. Lieberman, and G. H. Bernstein, *J. Vac. Sci. Technol. B* **22**, 1711 (2004).

²¹H. Namatsu, K. Yamazaki, and K. Kurihara, *J. Vac. Sci. Technol. B* **18**, 780 (2000).

²²H. F. Yang, A. Jin, Q. Luo, C. Gu, and Z. Cui, *Microelectron. Eng.* **84**, 1109 (2007).